Industrial Crops & Products 227 (2025) 120812

Contents lists available at ScienceDirect

Industrial Crops & Products

journal homepage: www.elsevier.com/locate/indcrop

Combustion enhancement and emission reduction in an IC engine by adopting ZnO nanoparticles with calophyllum biodiesel/diesel/propanol blend: A case study of General Regression Neural Network (GRNN) modelling

M. Srinivasarao [a,b], Ch. Srinivasarao [c], A. Swarna Kumari [d], Bikkavolu Joga Rao [e], Pullagura Gandhi [f], Seepana PraveenKumar [g], Olusegun D. Samuel [h,j,*], Ahmad Mustafa [i], Christopher C. Enweremadu [j], Noureddine Elboughdiri [k]

[a] Department of Mechanical Engineering, JNTUK, Kakinada, Andhra Pradesh, India
[b] Sanketika Vidya parishad engineering college, Visakhapatnam, India
[c] Department of Mechanical Engineering, KHIT, Guntur, Andhra Pradesh, India
[d] Department of Mechanical Engineering, UCEK, JNTUK, Kakinada, Andhra Pradesh, India
[e] Department of Mechanical Engineering, Godavari Global University, Rajamahendravaram 533296, India
[f] Department of Mechanical Engineering, GITAM (Deemed to be University), School of Technology, Visakhapatnam 530045, India
[g] Department of Nuclear and Renewable Energy, Ural Federal University Named After the First President of Russia Boris Yeltsin, 19 Mira Street, Ekaterinburg 620002, Russia
[h] Department of Mechanical Engineering, Federal University of Petroleum Resources, P.M.B, Effurun, Delta State 1221, Nigeria
[i] Center of Excellence, October University for Modern Sciences and Arts (MSA), Cairo, Egypt
[j] Department of Mechanical, Bioresources and Biomedical Engineering, University of South Africa, Science Campus, Private Bag X6, FL 1709, South Africa
[k] Chemical Engineering Department, College of Engineering, University of Ha'il, P.O. Box 2440, Ha'il 81441, Saudi Arabia

ARTICLE INFO

Keywords:
Calophyllum oil
Biodiesel
Propanol-2
Zinc oxide nanoparticles
IC engine
Generalized Regression Neural Network

ABSTRACT

Even though higher alcohols (HAs) and nanoparticles have the tendency to enhance engine behaviours (EBs), namely performance, emissions, and combustion characteristics, and ensure a greener environment, the absence of a reliable model to predict and model the appropriate HA dosage to blend with nanoparticles in green diesel (GD) has affected the biodiesel and automotive industries. For the first time, a study adopted a generalized regression neural network (GRNN) to investigate the influence of propanol-2 as one of the HAs, zinc oxide (ZnO) as one of the nanoparticles, and Calophyllum biodiesel (CB) as GD on EBs. The study focused on the effect of adding propanol-2 and ZnO fuel enhancers on the engine features and performance, combustion, and emissions of a CB blend (CB20) in an internal combustion (IC) engine. The results showed improved engine performance, with brake thermal efficiency increasing by 0.06 %, 1.71 %, and 3.91 %, and specific fuel consumption reduced by 5.83 %, 7.4 %, and 11.53 %, respectively, compared to CB20 fuel. The highest cylinder pressure of 70.84 bar was observed at the 120 ppm nano additive blend, while the highest heat release rate (HRR) of 36.65 J/°CA was observed at the same concentration of nano additives. Furthermore, the inclusion of ZnO nano condiments caused a decrease in carbon monoxide (CO), hydrocarbon (HC), nitrogen oxide (NOx), and smoke emissions by 38.7 %, 14.9 %, 4.8 %, and 2.48 %, respectively, at higher dosages of nano additives in the CB20 blend. A computational model based on a GRNN was constructed for further analysis of engine efficiency and emissions behaviour. The GRNN model accurately predicted output variables for various blends, with correlation coefficient (R) values varying from 0.98284 to 0.99959, with lesser RMSE and MAPE values within acceptable

DOI of original article: https://doi.org/10.1016/j.indcrop.2024.120386.

Abbreviations: BTE, Brake thermal efficiency; CT, Charge temperature; CP, Cylindrical pressure; EL, Engine load; EGT, Exhaust gas temperature; EPT, Fuel preheating temperature; GRNN, Generalized Regression Neural Network; HRR, Heat release rate; HC, Hydrocarbon carbon; IP, Injection pressure; IT, Injection timing; MAPE, Mean absolute percentage error; NA, Not adopted; NSGA, Non-dominated sorting genetic algorithm NSGA-II; PCA, Principal component analysis; RMSE, Root mean square error; SFC, Specific fuel consumption; TE, Thermal efficiency.

* Corresponding author at: Department of Mechanical Engineering, Federal University of Petroleum Resources, P.M.B, Effurun, Delta 1221, Nigeria.
E-mail addresses: samuel.david@fupre.edu.ng, olusegundavidsamuel@gmail.com (O.D. Samuel).

https://doi.org/10.1016/j.indcrop.2025.120812

Available online 14 March 2025

boundaries. The highest cylinder pressure of 70.84 bar was observed at the 120 ppm nano additive blend, while the highest heat release rate (HRR) of 36.65 J/°CA was observed at the same concentration of nano additives. Furthermore, the inclusion of ZnO nano condiments caused a decrease in carbon monoxide (CO), hydrocarbon (HC), nitrogen oxide (NOx), and smoke emissions by 38.7 %, 14.9 %, 4.8 %, and 2.48 %, respectively, at higher dosages of nano additives in the CB20 blend. A computational model based on a GRNN was constructed for further analysis of engine efficiency and emissions behaviour. The GRNN model accurately predicted output variables for various blends, with correlation coefficient (R) values varying from 0.98284 to 0.99959, with lesser RMSE and MAPE values within acceptable boundaries. The results also showed that the GRNN models are advantageous for network simplicity and require less data, making them reliable tools for predicting and modelling EP of the latest fuel for researchers and stakeholders in the automotive industry.

Nomenclature

BP	Blend percentage
BRSFC	Brake specific fuel consumption
NA	Not adopted
NC	Not considered
ND	Nanoparticle dosage
TOA	Types of additive

Greek symbols

σ	Smooth factor
X_i	Input vector of n variables per GRNN
Y_i	Output predicted by GRNN

1. Introduction

Fossil fuels have played a fundamental role in driving industrial growth for over a century, especially in transportation and power generation (Samuel et al., 2021); Tiwari et al., (2024)). However, the environmental challenges linked to fossil fuels, like air pollution and climate change, have emphasised the importance of realising cleaner and more sustainable energy sources (Abishek et al., 2024; Padmanabhan et al., 2024); Nema et al., (2023)). Biodiesel is an auspicious substitute to diesel, particularly for lower blends. It can be produced from a variety of oils, both edible and non-edible, such as palm oil, rubber seed, corn, canola, sunflower, soybean, jatropha, hemp, tobacco, rubber, and Sterculia foetida oil (Samuel et al., 2020; Devarajan and Selvam, 2024). The most common method for producing biodiesel is transesterification using ethanol or methanol with catalysts (Pradeep and Jogarao, 2020). While biodiesel offers several advantages over traditional diesel fuel, including its eco-friendly nature, oxygenation, non-toxicity, higher cetane rating, and biodegradability, experts recommend utilizing non-edible oil sources (Kumar et al., 2024). These sources consist of waste cooking vegetable oils, Jatropha curcas, Pongamia pinnata, cottonseed, and Calophyllum oil to prevent endangering food supplies and promote sustainability. Among the oils, Calophyllum oil (CaO) has appeared attractive for green diesel development and has been found to have similar fuel properties to fossil diesel, the highest oil yield, better engine performance, and emission attributes (Mosarof et al., 2016; Jain et al., 2018).

The Calophyllum tree belongs to the family of mangosteen or Clusiaceae and is plentiful in East Africa, India, South East Asia, Australia, and the South Pacific (Atabani et al., 2014). The yield of Calophyllum inophyllum oil (CIO) consistent with unit land area has been reported to be higher than 4 t/ha.

The CIO content of the seed is in the range of 40–73 %. Calophyllum inophyllum yields about twice as much oil per hectare as Jatropha curcas (Ong et al., 2011; Atabani et al., 2014). However, the extracted oil cannot be directly used in IC engines as there is evidence of degumming, injector chocking, and other IC engine malfunctions if CIO is used directly. Hence, transesterification is considered the best route to produce green diesel with enhanced fuel-related properties and higher yield compared to pyrolysis and emulsification processes in the biodiesel and automotive sectors. Biodiesel has drawbacks like inferior heating value, high viscosity, and high density, which make it difficult to use in higher blends. Addressing technical and economic challenges is crucial, especially with higher biodiesel blends. These blends may not perform as well as diesel in a standard engine, requiring modifications in engine design or fuel formulation. Fuel formulation techniques aim to create blends with specific properties to enhance performance, efficiency, and environmental goals for different applications, such as internal combustion engines (Sheriff et al., 2020). Researchers have conducted studies on the influence of alcohol additives on fuel blends. Rajendran and Govindasamy (2021) studied the effect of isopropanol alcohol (IPA) on blends of methyl ester of rubber seed oil (RSOME) at different compression ratios. Adding 5 % IPA to B10 resulted in a 3.14 % upsurge in brake thermal efficiency. Additionally, the addition of IPA to RSOME reduced carbon monoxide, hydrocarbon, and smoke emissions by up to 10.8 %, 33 %, and 32.2 %, respectively. Nour et al. (2019) studied the impact of pentanol and octanol on a hydrous ethanol/diesel blend. The results showed that octanol had lower brake-specific energy consumption (BSEC) and brake-specific fuel consumption (BRSFC) compared to diesel, while pentanol additives had higher values. Octanol also exhibited higher brake thermal efficiency (BTE) than diesel, whereas pentanol had lower BTE. The study found a significant decrease in smoke, NOx, CO, and CO_2 emissions by 73 %, 33 %, 83 %, and 56 %, respectively. Singh et al. (2020) studied the influence of adding 5 %, 10 %, and 15 % butanol to a eucalyptus biodiesel blend (B20). They detected that higher butanol concentrations led to a decrease in BRSFC compared to B20, although it was still slightly higher than automotive gas oil. Brake thermal efficiency (BTE) improved with increasing butanol content. The addition of butanol reduced NOx emissions but augmented CO2 emissions compared to diesel.

Nanomaterials (NMs) are increasingly being adopted as efficient octane boosters in diesel engines. Nano fuels are created by blending NMs with core fuels such as pure diesel, biodiesel, oil, diesel/biodiesel blends with emulsified water, and various alcohols like ethanol and butanol. The universally used NMs for this purpose are cerium dioxide, aluminum oxide, titanium oxide, copper oxide (Jayanthi and Rao, 2016), zinc and iron oxides, and carbon nanotubes (Pullagura et al., 2023). These materials have been shown to enhance the diesel engine performance by improving combustion efficiency and reducing emissions (Abishek et al., 2024b). Table 1 provides a brief overview of NMs in biodiesel to enhance internal engine behaviours (ICEB)

1.1. Exploration of GRNN technique in IC engines and other engineering applications

Stakeholders, scientists and researchers have employed the GRNN approach to study, investigate and monitor IC engines operated on diverse fuels while others have explored the aforementioned approach in sphere engineering application. For instance, a concise report on GRNN based study of engine operated on diverse fuels aims to boost the suitability of low carbon fuel, model and predict performance features in various engines. Table 2 highlights the report of GRNN-based prediction

of the effectiveness of fuels operating in engines. For instance, Simarouba biodiesel (Nithyananda et al., 2023), castor oil; ethanol, diesel fuel (Aengchuan et al., 2022), Mahua oil biodiesel doped with ZnO nanoparticle (Seela et al., 2018), ethanol fuelled HCCI engine (Bendu et al., 2016), natural gas (McLellan, 2007). Additionally, GRNN with or without its counterpart modelling tool is also explored in other engineering applications as indicated in Table 3. For instance, methanol synthesis factory (Wolday and Ramteke, 2024), estimation of CO_2 emission in China (Yue and Bu, 2023), predicting chemical exergy of technical lignin (Huang et al., 2022), mechanical features of hypereutectoid steel (MFHS) (Qiao et al., 2020), predicting crude oil expenses (Caraka, 2017), wind pressure data renovation (Ni and Li, 2016), pattern recognition (Polat and Yıldırım, 2008), observing batch processes (Kulkarni et al., 2004). The results of application of the tools have been showed to be suitable.

1.2. Fundamental theory of GRNN

The theory of the Generalized Regression Neural Network (GRNN) is based on non-linear regression estimation commonly used in statistics. This concept has enabled GRNN to possess exceptional multivariable plotting capability and a flexible network assembly (Qiao et al., 2020; Ni and Li, 2016; Celikoglu, 2006; Celikoglu and Cigizoglu, 2007). Prediction accuracy tends to be high with small sample data (Rooki, 2016; Xie et al., 2019).

GRNN was created as a substitute to the radial basis function neural network (Montazer et al., 2018). GRNN is a feed-forward neural network that relies on nonlinear regression theory. It features a simple and direct training algorithm, setting it apart from BPNN. Fig. 1 depicts the schematic of GRNN. The GRNN model comprises four components: the input layer, pattern layer, summation layer, and output layer. The input layer transmits training patterns and is linked to the pattern layer through weighted connections. The output from the pattern layer is then passed to the summation layer, which includes two types of units: denominator units and numerator units. The summation layer has a single denominator unit that calculates the unweighted sum of outputs from the pattern layer. The numerator units calculate the weighted sum of pattern layer outputs, with the weight being the value of the dependent variable for the training case of that pattern layer unit (Ni and Li, 2016). The number of numerator units equals the number of outputs. The output layer divides the output of each numerator unit by the output of the denominator unit. This logic can be summarized in a nonlinear regression formula as shown in Eq. (1).

$$E[|Y|X] = \frac{\sum_{i=1}^{n} Y_i \exp(-(X-X_i)^T \quad (X-X_i)/2\sigma^2}{\sum_{i=1}^{n} \exp(-(X-X_i)^T \quad (X-X_i)/2\sigma^2} \tag{1}$$

*Acronym appended in the nomenclature.

1.3. Gaps in knowledge, uniqueness, enthusiasm, and objectives of the study

A review of the literature highlighted Tables 2 and 3, as well as publications, indicating that several binary and ternary fuels have been used to run IC engines. Have previous empirical and stochastic technologies been employed to forecast and model the performance attributes, emission features, and combustion characteristics of diverse types of fuels in IC engines and other engineering sectors, from the standpoint of hypotheses?

The current empirical and stochastic technologies have not delivered a reliable forecasting model. There is a need for a resilient, self-learning,

Table 1
A concise revise of NMs in biodiesel for enhancing ICEB.

Types of NMs	Core fuels with NMs	Emulsified water, and various alcohols	Impacts on ICEB	Remarks	Refs.
Copper oxide	Karanja and safflower biodiesel (KB)	NA	BP increased by 8 % across all operation speeds and blend percentages, with KB40N generating the highest noise levels during combustion.	The incorporation of Copper oxide Nm improved the engine's combustion, performance characteristics	Kanimozhi et al. (2023)
TiO2	Mahua biodiesel	NA	A reduction of 4 % in NOx emissions was observed with blended biodiesel, and a 2.3 % reduction was achieved with nanoparticle-based blended biodiesel.	Reduction in emission features and enhanced combustion parameters	Sarma et al. (2023)
Titanium oxide (TiO2)	Pongamia biodiesel (POB)	NA	The addition of TiO_2 in POB increases combustion features, while reducing HC and NOx emissions.	ImMajor ICEB were enhanced	Rangabashiam et al. (2023)
copper oxide (CuO_2)	Neochloris oleoabundans methyl ester (NOME): NOMEB20, NOMEB20 + 25 ppm, NOMEB20 + 50 ppm, NOMEB20 + 75 ppm, and NOMEB20 + 100 ppm.	NA	Improved combustion, performance characteristic and decreased in exhaust emissions detected with the NMs explored	Major ICEB were enhanced	Kalaimurugan et al. (2023)
cerium-oxide (CeO_2)	Mahua biodiesel blend (MB): MB20 + 50 ppm, MB20 + 100 ppm, MB50 + 50 ppm and MB50 + 100 ppm)	NA	Enhanced BTE and lower SFC, reduced emission features	BTE of MB20 + 100 ppm CeO2 ↑ by 1.8 with 1 % betterment in SFC; Reduction in emission profile compared to BO	Seela et al. (2019)
Aluminium oxide (AlO)	Mahua biodiesel (MB)	NA	Improved BTE and lower SFC, reduced emissions. The use of AlNP led to a 26.04 % decrease in HC emissions and a 48 % decrease in CO emissions, while also increasing peak pressure and reducing the ignition delay period.	Doping of AlO in MB enhanced the BTE and reduce CO, HC and smoke pollutants	Aalam and Saravanan (2017)

↑= increase

Table 2
Overview of GRNN based study of engine operated on diverse fuels.

Fuel adopted	TOA	Engine's types	GRNN	Input engine constrain	Engine emission features (EEs)	Performance features (PFs)	Combustion Characteristic (CCs)	Remarks	Refs.
Calophyllum oil biodiesel	ZnO nanoparticle	Water cooled, power 5.2 kW at 1500 r.p.m	√	Fuel blends, propanol−2 additive, load	CO, HC, NOx, Smoke	BP, BTE, BRSFC	HRR, CP	Compressive measured and GRNN- based predicted EEs, PFs, and CCs of an IC engine operated on ternary fuels are established.	Present study
Simarouba Biodiesel	NC	Water cooled, 600 bar, standard injector pump engine	√	BP, IP, IT, FPT	CO, CO_2, UHC, NOX	BTE, BRSFC	×	Performance parameters of IC engine provided by GRNN	Nithyananda et al. (2023)
Castor oil; ethanol, diesel fuel (D80E10C10)	NC	model Kirloskar TV1	√	Fuel type, Compression ratio (CR), Engine load (EL)	Emission profiles	BRSFC, BTE	In-cylinder pressure and degree of heat issue		Aengchuan et al. ((2022)
Mahua oil biodiesel	ZnO	5 HP diesel engine	√	Fuel types, ND	NO_x, HC, CO_2, CO	SFC, BTE	×	The suitability of GRNN in predicting PEPs and RFs established	Seela et al. (2018)
Ethanol	×	HCCI	√	CT, EL	UHC, CO, NO, smoke opacity	BTE, EGT	×	The PEPs and PFs were predicted within 2 % with GRNN	Bendu et al. (2016)
Natural gas	×	LM6000 combustion turbines	√		NOx	×	×	GRNN reported to improve emissions tracking to reduce cost and capable of performing for a period of 1 year + 8 months	McLellan (2007)

BP = blend percentage,

and consistent prediction model that can handle multiple inputs and responses in scientific, automotive, and biofuel industries.

The objective is to determine the best solutions with nominal computing effort. To the best of the authors' knowledge, a ternary combination of Calophyllum oil biodiesel/propanol doped with ZnO nanoparticles (COBPZnO) has not been tested on a diesel engine. Additionally, available studies present limited investigation and results on the performance and emission features, while the combustion characteristics of such a ternary combination of COBPZnO have not been thoroughly investigated. The novelty of this research lies in the potential of doping ZnO nanoparticles with the ignition improver alcohol propanol-2 to enhance cold starting problems by enriching the oxygen content for proper combustion. Furthermore, the novel COBPZnO combination is expected to enable effective engine operation without modification. Lastly, the study aims to utilize Generalized Regression Neural Networks (GRNNs) to predict engine behavior and correlate performance, emission, and combustion features with engine variables, ensuring resilient self-learning capacity, rapid convergence, high prediction accuracy, and consistent prediction outcomes.

The outstanding modelling and prediction abilities of the GRNN include the ability to resolve function approximation problems, independence from iterative training procedures, and the capability to approximate any capricious function between input and response directions using training datasets. Additionally, GRNN provides a consistent basis for the estimator to tend toward zero as the training set- size tends large.

This study investigates the combined effect of propanol-2 and ZnO-based additives on the performance, combustion, and emissions characteristics of Calophyllum biodiesel blends in an IC engine. While previous studies have shown that propanol-2 and ZnO-based additives can enhance the efficacy of biodiesel blends, limited research has explored their combined effect when used with Calophyllum biodiesel blends. Therefore, this study aims to address this gaps and provide insights into the synergistic effects of these additives when combined with Calophyllum biodiesel blends. Additionally, the authors have developed an empirical model using GRNN to effectively predict engine output responses.

In the present investigation, the influence of doping ZnO in Calophyllum biodiesel with propanol blend on a direct-injection engine manufactured by Kirloskar was investigated using varying fuel types (CB20, CB20P5, CB20P5ZnO40, CB20P5ZnO80,CB20P5ZnO120), and ZnO dosage (40, 80, 120 ppm). In summary, the current research contributes to the literature in the following ways:

- Influences of many variables (fuel types, nanoparticles dosages) on engine behaviour were discussed.
- A comprehensive study of the effective utilization, and environmental friendliness, and combustion characteristics of zinc oxide-Calophyllum biodiesel-propanol ternary combinations were conducted.
- The correlation between the measured and GRNN-predicted engine behaviour of the ternary fuels for enhancing the effectiveness of the diesel engine and ensuring a greener environment was documented.

2. Material and methods

For the purpose of producing Calophyllum oil methyl ester (COME/biodiesel from CO with methanol as the liquor and KOH as the catalyst, CO were acquired from a commercial oil shop in Chennai, India. The investigation engaged high-purity analytical grade chemicals and reagents, as exposed in Table 3, which were procured from an indigenous vendor in Chennai, India.

This section details the materials and methods used in the study, including the supply of ZnO nanoparticles as fuel additives, COME production from CO via transesterification, preparation of blended fuels, and engine testing. Fig. 2 illustrates the study's stages.

Table 3
Adoption of GRNN in human, scientific and engineering applications (HSEA).

HSEA	GRNN	Other modelling tool (s)	Remarks	Refs.
Methanol synthesis factory	√	*NSGA-II	Reduction of computational day achieved by GNN model	Wolday and Ramteke (2024)
Estimation of CO_2 emission in China	√	Fruit fly optimization algorithm (FFOA)	Targeted CO_2 predicted through GRNN-FFOA models	Yue and Bu (2023)
Prediction of chemical exergy of technical lignin	√	×	Accuracy of GRNN model proven as the error are less than ± 0.15 %	Huang et al. (2022)
Mechanical features of hypereutectoid steel (MFHS)	√	K-folder cross validation (K-CV	The GRNN model predicted suitable results	Qiao et al. (2020)
Predicting crude oil expenses	√	×	Precise prediction obtained by GRNN model	Caraka (2017)
Wind pressure data renovation	√	BPNN	Reconstruction of wind pressure dataset achieved by GNN	Ni and Li (2016)
Pattern recognition	√	Genetic algorithm (GA)	Efficacy of optimized GRNN showcased over non-optimized scenario	Polat and Yıldırım (2008)
Observing of batch processes	√	*PCA	Demonstration of the effective monitoring proven by GNN and PCA technique	Kulkarni et al. (2004)

√ = available, × = unavailable; Acronym appended in the nomenclature.

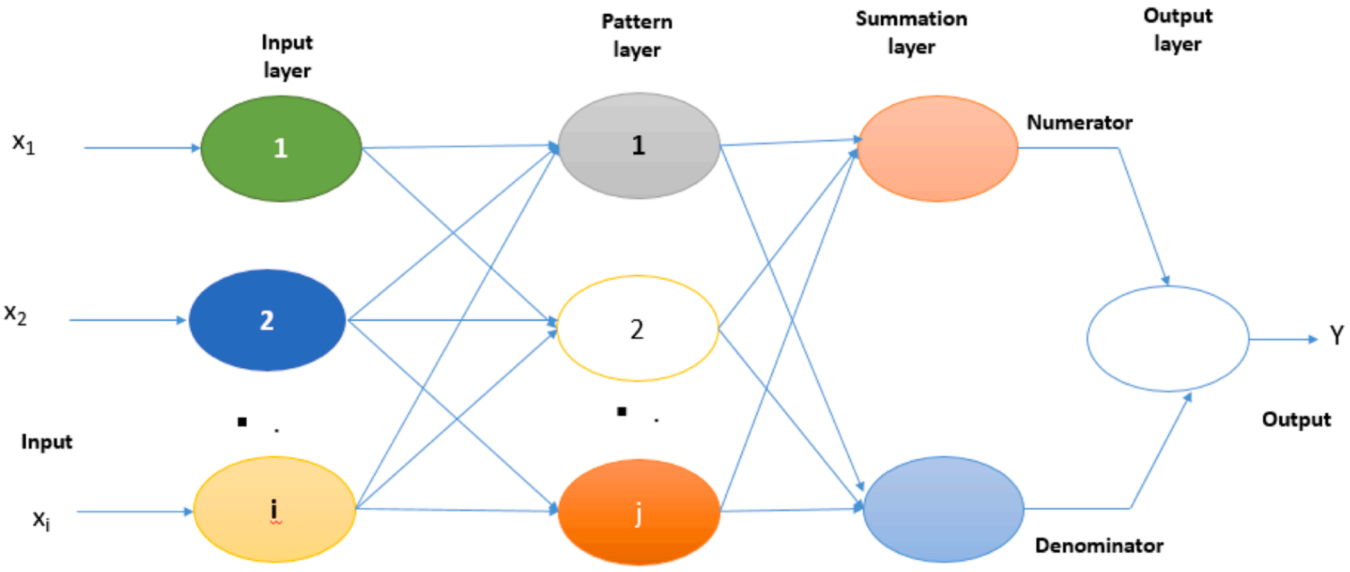

Fig. 1. The general schematic of GRNN.

2.1. Preparation of COME

Fig. 3 portrays the preparation of COME. As shown, to prepare COME, a mixture of 18 g of KOH catalyst and 250 ml of methanol is used and then added to the pre-treated CO, which is heated to 60 °C using a heating coil and stirred with a mechanical stirrer. The temperature was maintained below 60 °C to prevent the methanol from evaporating. The solution (KOH-methanol) is vigorously stirred for two hours and then transferred to a glass container to separate the COME the glycerine. The glycerine is removed, and the COME is cleaned with water to eradicate any remaining glycerine. The washing process is repeated until no glycerine is left. Finally, the purified biodiesel is heated to 100 °C to remove any water content, resulting in a high-quality biodiesel product ready for nano blend preparation.

2.2. Preparation of fuel additive: COME and ZnO nanoparticle blend

Fig. 4 depicts the method employed to produce ZnO nano blend fuel. Initially, 200 ml of COME was taken, and then 5 % (50 ml) of propanol-2 was added to a magnetic stirrer for 20 minutes. After that, ZnO nanoparticles were measured in adequate quantities of 40, 80, and 120 ppm using a precise weighing scale. These ZnO nanoparticles are dispersed in a mixture by ultra-sonication at 20 kHz for 30 min to prepare a nano blend. Therefore, the ZnO nanoparticles-infused fuels are abbreviated as CB20P5, CB20P5, CB20P5ZnO40, CB20P5ZnO80, and CB20P5ZnO120. The abbreviations of the test fuels obtained and information about the fuel components are given in Table 4. The properties of reformulated fuels are characterised

2.3. Engine assessments

The prepared fuel blends CB20P5, CB20P5ZnO40, CB20P5ZnO80, and CB20P5ZnO120, as well as the DF used as along with the reference fuel DF, were tested at varying different loads (25 %, 50 %, 75 %, and 100 %) in a 1-cylinder, 4-stroke, VCR Engine (computerized) with pre-installed engine software on a PC. Engine performance, combustion, and exhaust emission measurements were carried outs were measured. The tests were conducted on a water-cooled engine with a power rating of 5.2 kW at 1500 rpm, a direct-injection engine manufactured by the Kirloskar brand as shown in Fig. 5. Table 5 highlights The technical specifications of the engine used in the test setup.

2.3.1. Experimental setup and mode of operation

A combination of RTD, PT 100, and K-type thermocouples are used to measure engine water and exhaust temperatures in different temperature ranges. Combustion and fuel inlet pressures are measured using

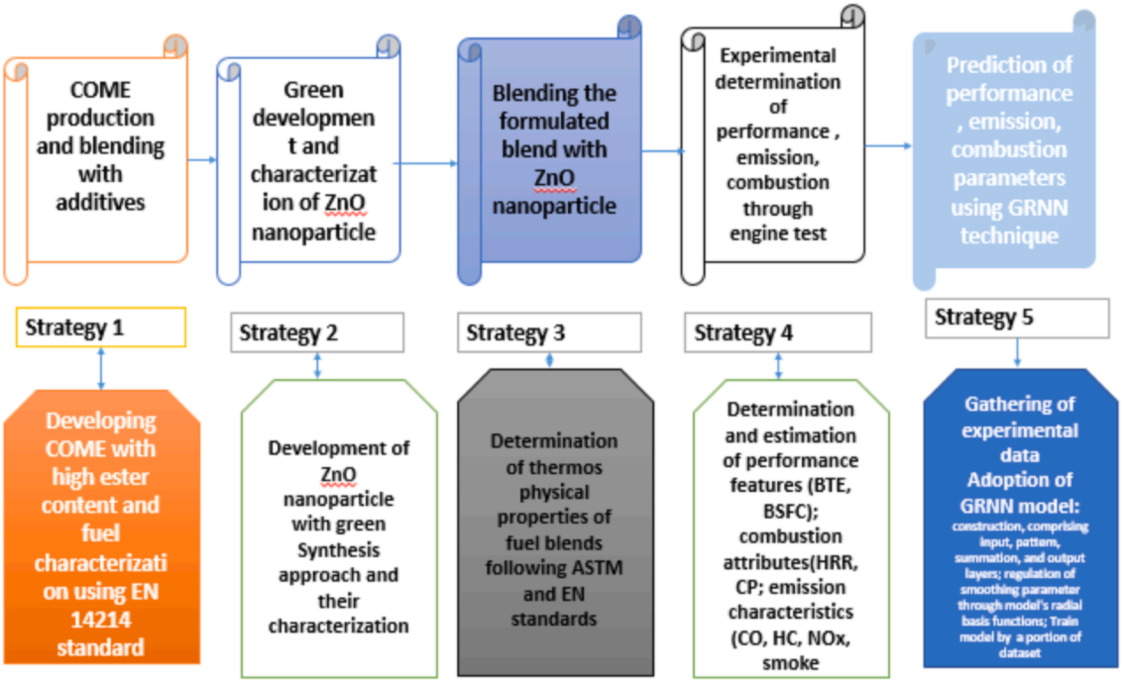

Fig. 2. Diagram showing the modified stages of the research.

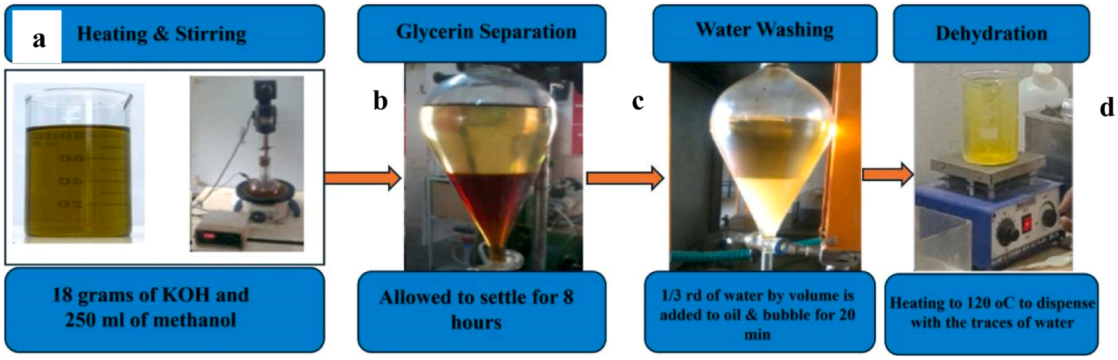

Fig. 3. Preparation of biodiesel from Calophyllum crude oil: (a) heating and stirring, (b) glycerin separation, (c) water washing, (d) dehydration.

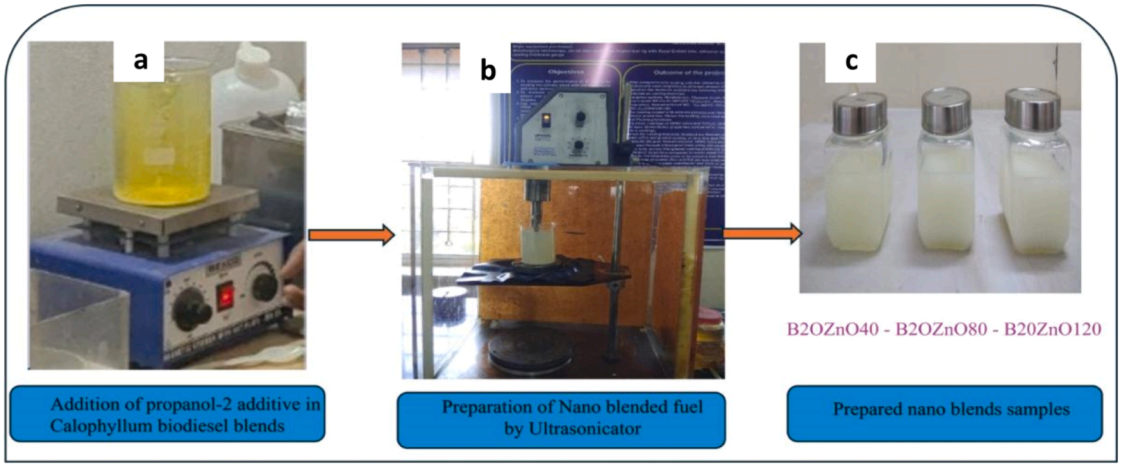

Fig. 4. Process for the preparation of nano blend samples: (a) addition of propanol-2 additive in calophyllum biodiesel blends, (b) preparation of nano-blended fuel by ultrasonication, (c) prepared nano blended samples.

Table 4
Test fuels.

CB20	CB20P5	CB20P5 ZNO40	CB20P5ZNO80	CB20P5ZNO120
20 % of Biodiesel blended in 80 % of Diesel	20 % of Biodiesel + 75 % of Diesel+ 5 % of Propanol	20 % of Biodiesel + 75 % of Diesel+ 5 % of Propanol+ZnO nanoparticles at a dosage of 40 ppm	20 % of Biodiesel + 75 % of Diesel+ 5 % of Proponal+ZnO nanoparticles at a dosage of 80 ppm	20 % of Biodiesel + 75 % of Diesel+ 5 % of Proponal+ZnO nanoparticles at a dosage of 120 ppm

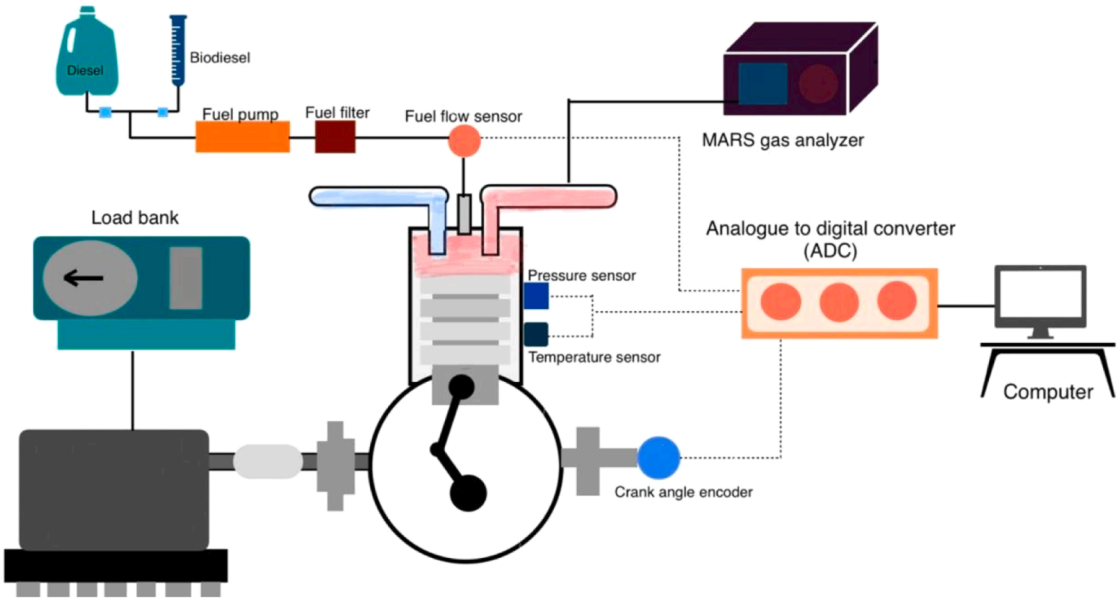

Fig. 5. Schematic setup of VCR Engine computerized diesel test bed.

Table 5
Detail of the test engine and equipment.

Specifications	Descriptions
Product	1 cylinder, 4 stroke, VCR Engine (Computerized)
Rated power	5.2 kW at 1500 rpm
Bore and Stroke	87.5 mm and 110 mm
Compression ratio	16:1, 17.5:1 and 19:1
Loading	Eddy Current Dynamometer
Load sensor	Load cell, type strain gauge
Temperature sensor	Type RTD, PT100 and Thermocouple, Type K
Fuel flow transmitter	DP transmitter, Range 0-500 mm WC
Airflow transmitter	Pressure transmitter, Range (-) 250 mm WC
Rotameter	Engine cooling 40-400 LPH; Calorimeter 25-250 LPH
Software	"Enginesoft" Engine performance analysis software
Data acquisition device	NI USB-6210, 16-bit, 250kS/s.

piezoelectric sensors with a low-noise cable, with a range of 5000 PSI. The piezoelectric sensor converts pressure into electrical signals for human-readable display. The control panel houses a 15 L fuel tank, an air box, a manometer, a fuel burette, a Denso fuel pump, and injector with a pressure of 220 bar, and a Yokogawa fuel flow transmitter. The engine is connected to a water-cooled SAJ eddy current dynamometer for load measurement using a strain gauge-type load cell and a rotary encoder for speed measurement. All sensors are linked to the data acquisition system. The compression ratio can be adjusted using a tilting block arrangement without altering the combustion chamber. Emissions are analyzed using a Mars portable five-gas analyzer and smoke meter by inserting an analyzer probe into the engine's exhaust pipe.

2.3.2. Error analysis and uncertainties

Errors and uncertainties in tests may arise from equipment selection, personal observations, conditions, atmosphere, readings, and test preparation (Samuel et al., 2021). Error analysis is crucial for ensuring the accuracy of the test results. Uncertainty assessment is vital in complex experiments.

Identifying and rectifying common mistakes can enhance the precision experimental outcomes. Conducting repeated tests can aid in errors elimination. The total uncertainty of the examination apparatus is determined by talking into account all performance variable errors, as shown in Table 6.

$$\sqrt{SFC^2+BTE^2+HRR^2+CP^2+CO^2+HC^2+NOx^2+Smoke^2}$$

$$\sqrt{0.55^2+\ 0.26^2+\ 1^2+\ 1^2+\ 1.5^2+\ 0.15^2+\ 1^2+\ 0.15^2}$$

$$\sqrt{0.3025+0.0676+1+1+\ 2.25+\ 0.0225+1+\ 0.0225}$$
$$=\pm 2.3801$$

2.4. GRNN modelling

The analysis of biodiesel blends with fuel additives using a GRNN commences with gathering experimental engine data. Fig. 6a illustrates the GRNN design. The GRNN architecture, as displayed, consists of four

Table 6
Accuracy and uncertainty of instruments.

Measured quality	Measuring range	Resolution	Uncertainty
CO	0–15 %	0.01 % vol	± 1.5%
CO_2	0–20 %	0.01 % vol	± 0.15%
HC	0–3000 ppm	≤ 2000: 1 ppm > 2000: 10 ppm	± 0.15%
O_2	0–25 %	0.01 % vol	± 0.5%
NO	0–5000 ppm	1 ppm	± 1 %
Smoke	0–100%	0.1 %	± 0.15%
Engine Speed	400–6000 min^{-1}	1 min^{-1}	± 1 %
Oil Temperature	0–125 °C	1 °C	± 4%

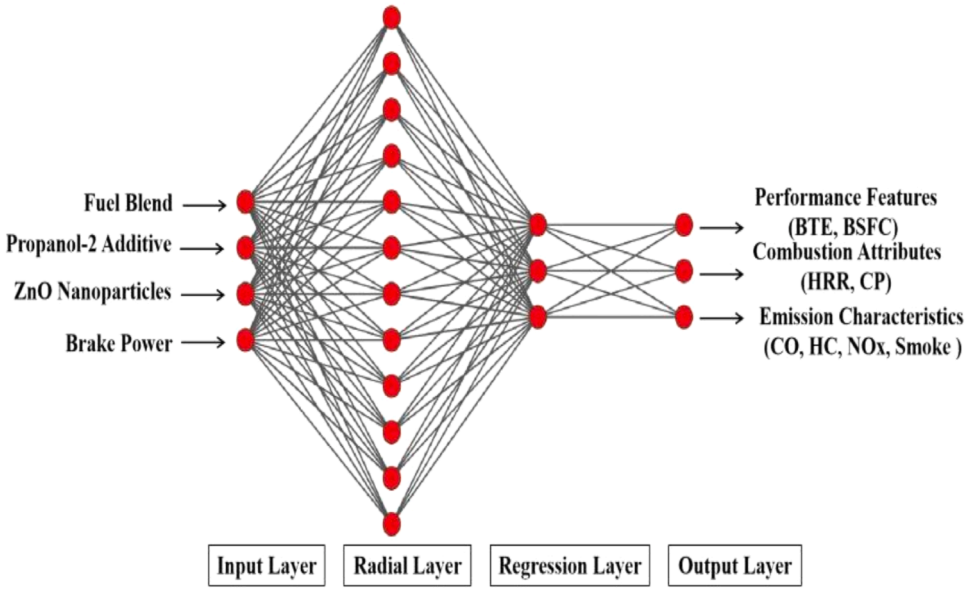

Fig. 6a. GRNN Architecture.

input variable with, and a four features in the output responses. As illustrated, this data encompasses input variables (BP, biodiesel blend ratios, Propanol-2 concentration, and ZnO additives) and output (BRSFC, brake thermal efficiency, CO, HC, NOx, smoke, cylinder pressure, and heat release rate).

Fig. 6b presents the flow chart for GRNN based modelling of the novel ternary fuel operated on IC engine. As depicted, the collected data undergoes preprocessing, which involves cleaning and normalization, followed by the identification of crucial input and output parameters. The GRNN model is then constructed, comprising input, pattern, summation, and output layers. The model's radial basis functions are regulated by the smoothing parameter (sigma). A quota of the dataset is adopted to train the model, while the lasting data is utilised for testing its performance. The model's accuracy is evaluated using performance metrics such as RMSE, MAPE, and R^2, comparing predicted results with experimental data. The analysis reveals how propanol-2 and zinc oxide additives impact engine performance and emissions. The study concludes by assessing the model's predictive capabilities and highlighting the additives' effects on engine behaviour.

2.4.1. Evaluation of performance metrics for the GRNN model using statistical methods

Statistical variables such as regression coefficient (R^2), Mean Relative Error (MRE), and Root Mean Square Srror (RMSE) were explored to detect the predictive superiority of the model techniques. Eqs. (1)– (3) were employed to evaluate the statistical metrics of the GRNN models. The results were used to assess the feasibility of GRNN in predicting the effectiveness of IC engine and the feasibility of fuel enhancement for a greener environment.

$$R^2 = 1 - \left\{ \frac{\sum_{i=1}^{n} (E_i - P_i)^2}{\sum_{i=1}^{n} (P)^2} \right\} \quad (1)$$

$$\mathrm{MRE}(\%) = \frac{1}{n} \sum_{i=1}^{n} \left| 100 \quad \frac{E_i - P_i}{P_i} \right| \quad (2)$$

$$\mathrm{RMSE} = \sqrt{\frac{1}{n} \sum_{i=1}^{n} (E_i - P_i)^2} \quad (3)$$

Where E_i, P_i,n = are the experimental data, predicted value, number of data values, respectively.

3. Result and discussions

3.1. Basic properties of fuel and analysis of ZnO additive

Table 7 presents the basic properties of fuel, namely Calophyllum oil-ethanol- doped with ZnO nanoparticles (NPs) (COME-P-ZnO), specifically CB20P5, CB20P5 ZNO40, CB20P5ZNO80, CB20P5ZNO120, 20 % COME (CB20), and diesel fuel (B0). The kinematic viscosity (KV) of CB20P5 (2.877 mm^2/s), CB20P5 ZNO40 (2.67 mm^2/s), CB20P5ZNO80 (2.69 mm^2/s), CB20P5ZNO120 (2.72 mm^2/s), and CB20 (2.91 mm^2/s) is marginally higher than that of B0 (2.557 mm^2/s) but falls within the ranges specified by ASTM D6751 (1.9–6.0 mm^2/s). There's no need to adjust the diesel engine due to the negligible difference in kinematic viscosity between COME-P-ZnO and B0 (Permude et al., 2012).

The density of CB20P5 (827 kg/m^3), CB20P5 ZnO40 (832 kg/m^3), CB20P5ZnO80 (840 kg/m3), CB20P5ZnO120 (857 kg/m3), and CB20 (842.5 kg/m^3) is marginally higher than B0 (830 kg/m^3). The higher density in COME-P-ZnO compared to B0 suggests that the fuel will have minimal impact on specific fuel consumption and penetration when injected (Sayin et al., 2012).

The flash point (FP) of all COME-P-ZnO samples is higher than B0 and meets ASTM D6751 safety standards. Fuels with higher flash points are less likely to catch fire compared to B0 (Bhuiya et al., 2016).

The calorific values (CAV) of CB20 (40452.34 kJ/kg), CB20P5 (41402.94 kJ/kg), CB20P5 ZNO40 (41448.23 kJ/kg), CB20P5ZNO80 (41493.28 kJ/kg), and CB20P5ZNO120 (41528.46 kJ/kg) are somewhat inferior to B0 (42500 kJ/kg). This slight reduction in CAV for all COME-P-ZnO blends compared to B0 indicates that the fuel might prone to an upsurge in BRSFC and could be slightly more economical for powering IC engines (Singh et al., 2015).

The ultraviolet absorption spectra (UVAS) and transmission electron microscopy (TEM) are displayed in Fig. 7(a-b). As portrayed in Fig. 7a, the UVAS range falls between 360 and 700 nm, with absorbance confirmed at 364.36 nm. Similar observations were reported by Talam et al. (2012) for Zinc nitrate nanoparticle UVAS. The TEM images provide high-magnification views of the sample's internal structure, revealing data on internal cracks, stress, crystalline structures, and contaminants. The TEM image at 100 nm is displayed in Fig. 7b. The

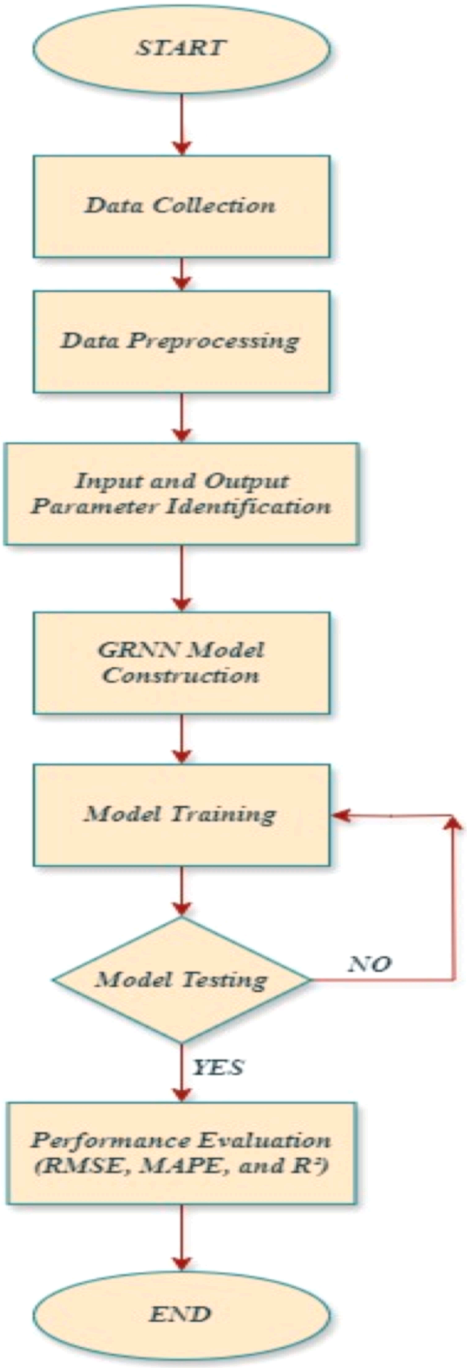

Fig. 6b. Flow chart for GRNN model for a novel ternary fuelled IC engine.

ZnO nanoparticle of mean particle size in the bound of 300–50 nm with bulk density varying from 0.28 to 0.48 g/cm^3, were donated by nano research lab Jharkhand-832102, India with detailed specifications as listed in Table 8. Related physical properties of ZnO nanoparticles adopted concurred with those indicated elsewhere (Rajak et al., 2023).

3.2. Performance characteristics

Fig. 8(a-b) illustrates the relationship between brake thermal efficiencies (BTEs) and specific fuel consumption (SFC) in relation to brake power (BP). The experiments were conducted at brake powers ranging from 1.29 to 4.89 kW. The BTEs of fuel types such as COME-P-ZnO and CB20 were lower than B0, attributed to their lower calorific value (Hosseini et al., 2017). However, the BTEs of CB20P%Zn0120 > CB20P %Zn080 > CB20P%Zn040 > CB20P%ZnP5, indicating that fuels with higher ZnO nanoparticle content exhibited enhanced BTE. This improvement can be attributed to the oxygen molecule donation by the nanoparticles during combustion, aiding in the breakdown of carbon compounds and promoting better combustion. The nanoparticles also demonstrated high catalytic activity, enhanced atomization, abridged ignition delay, and minimized heat wastage, resulting in improved BTE (Suhel al., 2021; Shaafi et al., 2015). Similar trends in BTE for fuel doped with nano additives have been observed in former studies (Gavhane et al., 2020; Simhadri et al., 2024).

The amount of fuel needed for an engine realise a unit power output is known as SFC. The SFC for B0, of fuel types such as COME-P-ZnO and CB20 at varying BP are depicted in Fig. 8b. SFC of B0 was detected to be inferior to all the DSOME-nanoparticles blends at all engine load situations. The SFC of all fuel types remains the same at the lowest load of 1.29 kW. However, at the higher load of 4.89 kW, the SFC of CB20P5ZnO 120 < CB20P5ZnO80 < CB20P5ZnO40 < CB20P5ZP5. The inclusion addition of ZnO NPs to the CB20 blend acts as the fuel catalyst, which results in the reduction in fuel consumption for achieving a similar engine power output. ZnO nanoparticle doped with CB20 possess a tendency to result in an oxygenated ternary fuel blend, resulting in less SFC due to low viscosity and density which results in the better air-fuel mixture and superior atomization. High evaporation reduces ignition delay, combusts excess fuel in the pre-mixed phase, and leads to increased power output and lower SFC (Nanthagopal et al., 2017). The lowest SFC was achieved with the 120-ppm infused CB20 fuel. However, for lower dosages of ZnO nanoparticles, SFC was higher due to particle aggregation, which reduces the ratio of surface area to volume and, as a result, diminishes the catalytic action of NPs (Soudagar et al., 2020). A similar pattern of SFC reduction with ZnO improver was studied by Dhahad and Chaichan (2020).

3.3. Emissions characteristics

Fig. 9(a-b) exemplifies the connection between carbon monoxide (CO) and hydrocarbon (HC) while Fig. 10 (a-b) demonstrates the relationship among oxide of nitrogen (NO_x) and smoke with respect to brake power. The experiments were conducted at brake powers ranging from 1.29 to 4.89 kW.

3.3.1. CO and HC emissions

Incomplete combustion, caused by an absence of oxygen, low combustion temperature, and a nearby rich fuel mixture in the combustion

Table 7
Thermophysical Properties of ternary oxygenated fuel.

Characteristics	ASTM D6751	Diesel	CB20	CB20P5	CB20P5 ZNO40	CB20P5ZNO80	CB20P5ZNO120
KV @40°C in mm^2/s	1.9–6	2.557	2.91	2.877	2.67	2.69	2.72
Density in kg/m^3	860–900	830	842.5	827	832	840	857
FP °C	> 130	45	61	50	67	69	70
Calorific Value kJ/kg	-	42500	40452.34	41402.94	41448.23	41493.28	41528.46

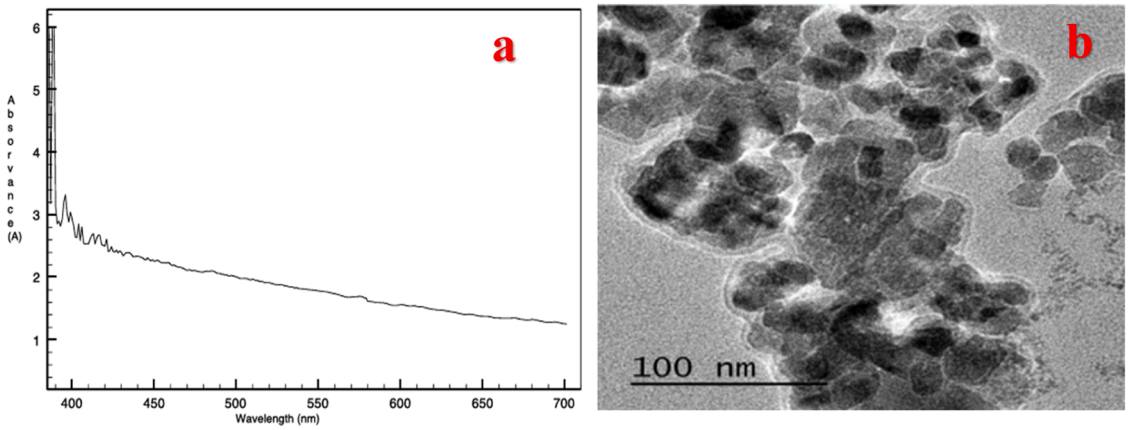

Fig. 7. Characterization tests: (a) UV-Vis Absorbance; (b) TEM at 100 nm.

Table 8
Physical properties of ZnO nanoparticles.

Name of the Product	Zinc Oxide Nanoparticles
Physical appearance	
Colour	Milky white
Form	Powder
Purity	99.9 %
Average Particle Size	30–50 nm
Morphology	Nearly spherical
SSA	20–60 m^2/g
Bulk Density	0.28–0.48 g/ cm^3
True density	6 g/cm^3
Molecular Weight	81.38 g/mol
Melting Point	1975 °C
Boiling Point	2360 °C
Thermal Conductivity	49 W/m-K
Specific Heat Capacity	0.494 J/g-°C
Thermal expansion	10–80 K

compartment, leads to the generation of CO emissions. Fig. 9a illustrates the variations in CO emissions at different loads for each sample. At full load, the CB20 blend exhibited a 42.74 % higher CO level compared to pure diesel. However, the blend with a 5 % propanol-2 fuel additive showed a 3.83 % decrease in CO emissions, which further decreased by 9.04 %, 5.47 %, and 12.87 % with the 40, 80, and 120 ppm nanoparticle fuel blends, respectively. The addition of propanol-2 reduces CO emissions, and the use of ZnO nanoparticle-based fuels further reduces CO emissions by disintegrating into Zn and O atoms during the combustion reaction. The O atoms enhance the oxidation proportion of fuel fragments, while Zn atoms improve the heat migration between the flame obverse and non-burnt fuel molecules, enhancing combustion. A comparable decrease in CO emissions with CNT NPs in neem biodiesel was reported by Ramakrishnan et al. (2019).

HC emissions are usually caused by the fuel failing to participate in the combustion reaction. Fig. 9b displays the discrepancies in HC emissions at altered loads for each sample. As load increases, HC emissions rise for all fuel types. This is due to excess fuel participating in combustion without increased air, resulting in a higher fuel-air mixture and more HC emissions (Manigandan et al., 2020). At full load conditions, CB20 has 31.57 % higher HC emissions than B0 owing to its advanced KV, which causes incomplete combustion and the generation of large droplets. Additionally, CB20 contains unbreakable, unsaturated hydrocarbons that contribute to higher HC emissions. HC emissions were significantly decreased by 15.78 % with propanol-2 fuel additive and also decreased by 14.91 %, 4.38 %, and 2.63 %, respectively, compared to the CB20 blend when 40, 80, and 120 ppm ZnO NPs were

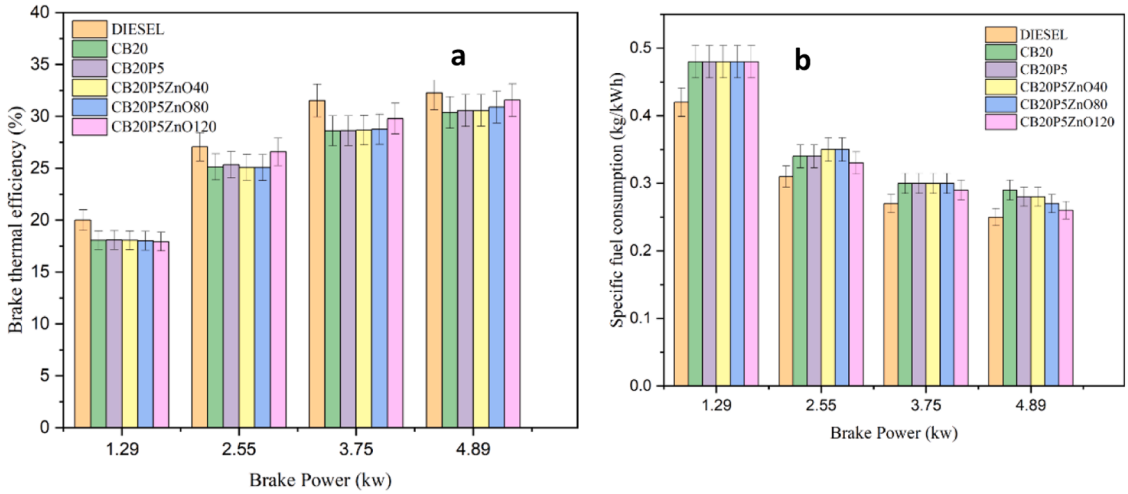

Fig. 8. Variation of BTE and SFC with brake power for novel ternary fuel: (a) BTE vs. BP and (b) SFC vs. BP.

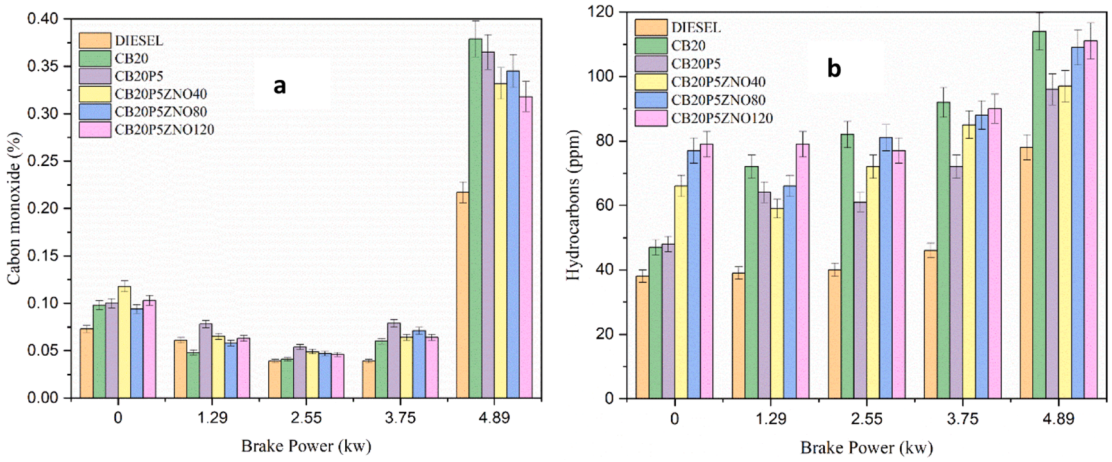

Fig. 9. Discrepancy of CO and HC with BP for novel ternary fuel: (a) CO vs. BP and (b) CO vs. BP.

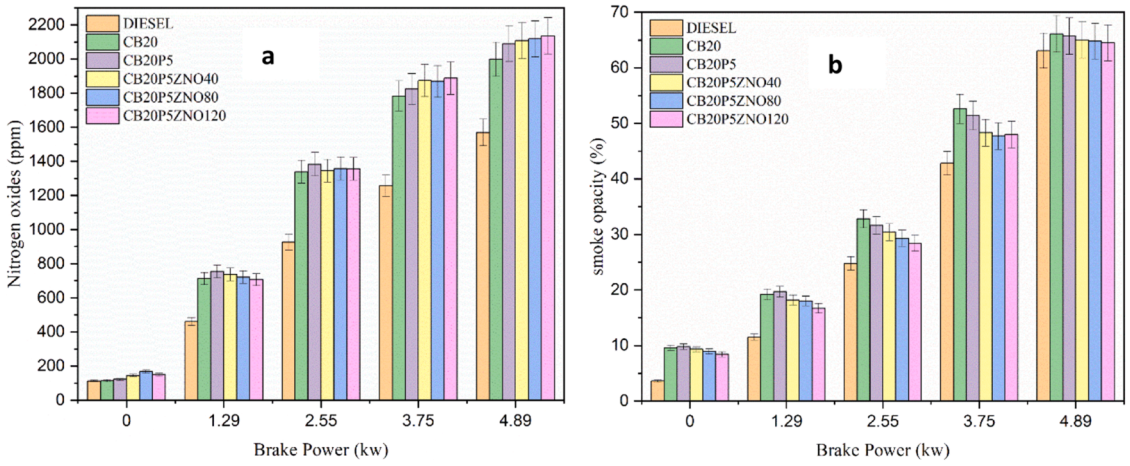

Fig. 10. Discrepancy of NOx and smoke opacity with BP for novel ternary fuel: (a) NOx vs. BP and (b) NOx vs. BP.

doped with CB20SPA50 blend. The nanoparticles release oxygen molecules throughout the combustion and have an enormous reactive surface, which helps oxidize unburned fuel elements and increase the evaporation degree. This results in fewer rich fuel zones in the combustion chamber and lower HC emissions (HCE). Hosseini et al. (2017) noticed a comparable reduction in HCE for waste oil-domiciled biodiesel with nanoscaled carbon nanotube molecules at different dosages.

3.3.2. NO_x and smoke emissions

Factors such as temperature, air-fuel combination, residence period, and fuel structure affect the formation of NOx in engines. Fig. 10a illustrates the impact of NO_x emissions based on the load of different fuel. The graph shows that all fuels exhibited an increasing trend in NO_x emissions as the load increased. At full load conditions, the CB20 blend had 21.47 % higher NOx emissions than diesel, and adding 5 % of propanol-2 and zinc oxide fuel additive blend increased the NO_x by 4.40 %, 5.21 %, 5.66 %, and 6.46 % respectively compared with the CB20 fuel blend. The increase is due to its high carbon content, which requires extra oxygen and period to break down, leading to higher in-cylinder temperature and hindered combustion. This study found a similar increasing trend in NOx emissions as reported by Gavhane et al. (2020) for copper-coated zinc oxide nanoparticles in soybean biodiesel

The smoke was primarily caused by the much reaction temperature, excess oxygen, and sufficient reaction period. Fig. 10b illustrates the impact of smoke on the load of each fuel. At full load, the CB20 blend showed 4.75 % higher smoke compared to pure diesel. However, the 5 % propanol-2 fuel additive blend reduced smoke by 0.6 %, and further reductions of 1.07 %, 1.38 %, and 1.86 % were observed with the 40, 80, and 120 ppm nanoparticle fuel blends. This shortage is attributed to the catalytic effect of NPs, which enhance combustion, shorten ignition delay, and provide oxygen during the combustion reaction. The O_2 in the ZnO structure are released during the premixed phase of combustion, accelerating the oxidation proportion of soot particles and resulting in less smoke. Soudagar et al. (2020) observed similar smoke patterns in their research on hybrid ZnO nano-fuel.

3.4. Combustion characteristics

The effects of COME-P-ZnO ZnO blends on combustion characteristics, such as in-cylinder pressure (ICP), heat release rate (HERR) and cumulative heat release are debated in the consequent sections. Fig. 11 (a-b) shows the connection between ICP and HERR against crank angle.

3.4.1. ICP and HERR

Cylinder pressure data is essential for monitoring engine combustion (El-Adawy, 2023). In a CI engine, the ICP in the combustion chamber is affected by the quantity of fuel involved in uncontrolled combustion. Different fuels exhibit varying ICP levels at complete load conditions with the crank angle, as depicted in Fig. 11a. The CB20 blend reduced ICP 2.50 % paralleled to B0. Conversely, the injection of a 5 % propanol-2 fuel additive blend and zinc oxide nanoparticles increased cylinder pressure by 3.81 %, 2.65 %, 0.26 %, and 0.11 %, respectively,

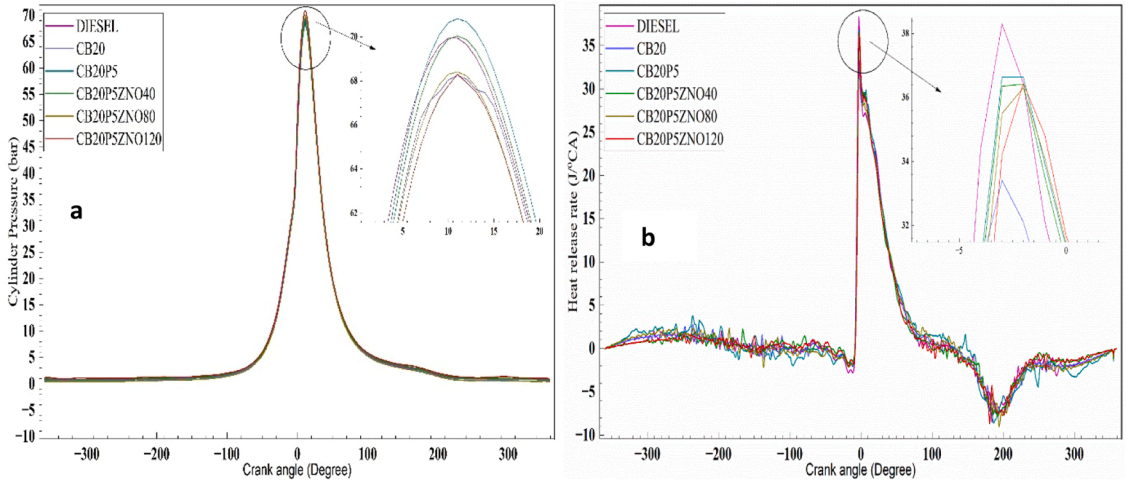

Fig. 11. Discrepancy of CP and HERR with crank angle (CA) for novel ternary fuel: (a) CP vs. CA and (b) HERR vs. CA.

compared to CB20. Nanoparticles, with their high surface-to-volume ratio, exhibit catalytic properties (Pullagura et al., 2023) and can also serve as an oxygen buffer (Rao et al., 2022), thereby enhancing the combustion process. Similar results regarding in-cylinder pressure have been reported by various researchers using nanoparticles and biodiesel (Kannan et al., 2011; Najafi, 2018).

The HERR is a crucial parameter that provides insights into the combustion progression in the engine cylinder. Fig. 11b illustrates the HRR versus crank angle for different fuels. Under full conditions, the HRR of the CB20 blend was 12.76 % lower compared to B0, ascribed to the diminutive ignition delay of biodiesel due to its greater cetane number. Additionally, biodiesel's high kV, surface tension, and poor atomization contribute to lower HRR. However, the addition of a 5 % propanol-2 fuel additive and zinc oxide nanoparticles increased the HRR by 9.66 %, 8.79 %, 6.25 %, and 2.36 %, respectively, compared to CB20. This HRR improvement is attributed to high-momentum liquid droplets and the catalytic action of zinc oxide nanoparticles, enhancing the combustion process for longer and more complete combustion than CB20. Bitire et al. (2023) observed a similar trend when the dosage of Cuo nanoparticles increased the HRR.

3.5. Application of GRNN modelling on experimental data

The GRNN models developed for analysing Calophyllum biodiesel blends with propanol-2 and zinc oxide-based fuel additives in internal combustion engines have demonstrated high accuracy in predicting various performance, combustion, and emissions parameters. This highlights their effectiveness in capturing the complex interactions within the engine system.

The model's performance and accuracy were assessed by matching the predicted outputs of the GRNN with the experimental values. Fig. 12 (a-h) displays the GRNN predictions for Brake Thermal Efficiency (BTE), SFC, Carbon Monoxide (CO), Hydrocarbons (HC), Nitrogen Oxides (NO_x), Smoke, Cylinder Pressure (CP), and Heat Release Rate (HERR) in comparison to the actual measured values. Furthermore, Table 9 shows the relationship between predicted and measured values for engine characteristics of novel ternary fuelled engines. Linear equations of $(0.9057x+2.4923)$ and $(1.000x-0.0028)$ were detected found for the change in GRNN predicted BTE and SFC versus measured BTE and SFC due to high regression coefficient (R^2) of 0.968 and 0.952. Fig. 12 (a-b) portrays the BTE model with an R of 0.99957, RMSE of 0.78047, MAPE of 2.69369 %, while the GRNN predictions for SFC achieved an R of 0.99919, RMSE of 0.01388, and MRE of 2.76923 %, underscoring the high accuracy of the BTE and SFC models in forecasting engine performance metrics. Linear equations of $(1.1743x - 0.0252)$, $(0.9025x - 7.5479)$,$(0.992x - 13.463)$, and $(0.9469x+2.1799)$ were identified suitable for the change in GRNN predicted CO, HC, NOx, and Smoke models versus measured values with high R^2 values. The GRNN based models effectively predicted emission traits including CO, HC, NOx, and smoke, as shown in Fig. 12 (c-f), with high R values and low RMSE and MAPE values, validating the precision of the RNNN models in predicting emission levels.

Linear equations of $(0.9515x+3.0399)$ and $(0.9124x+3.5766)$ were found suitable for correlating combustion features, namely CP and HHR models versus measured values due to high R^2 values Fig. 12 (g-h) further illustrates the high accuracy of the GRNN models in predicting CP and HRR, with low RMSE values and MAPE values.

Overall, these results highlight the effectiveness of GRNN analysis in modelling and predicting the complex interactions among fuel blends, additives, engine performance, combustion, and emissions, demonstrating the utility of advanced neural network models in optimizing engine operations and enhancing environmental sustainability through informed fuel formulation and combustion optimization strategies.

4. Conclusions

This study investigated the feasibility of adopting General Regression Neural Network (GRNN) in modelling and predicting performance characteristics, namely brake thermal efficiency (BTE) and SFC, emission features such as CO, NOx, Smoke, and combustion features such as combustion pressure (CP) and HERR of an IC engine fuelled with 20 % of Biodiesel blended with 80 % of Diesel (CB20), 20 % of Biodiesel + 75 % of Diesel + 5 % of Propanol (CB20P5), 20 % of Biodiesel + 75 % of Diesel + 5 % of Propanol + ZnO nanoparticles at a dosage of 40 ppm (CB20P5 ZnO40), 20 % of Biodiesel + 75 % of Diesel + 5 % of Propanol + ZnO NPs at a quantity of 80 ppm (CB20P5ZnO80), and 20 % of Biodiesel + 75 % of Diesel+ 5 % of Propanol + ZnO NPs at a quantity of 120 ppm (CB20P5ZnO120). To conduct a comprehensive study in the near future, the following aspects can be further investigated: (i) the impact of a novel ternary fuel spectrum, (ii) exergetic and exergoeconomic assessment of fuels used in IC engines, and (iii) vibration and acoustic characteristics of IC engines fuelled with various sizes of nanoparticles incorporated into the fuel. Additionally, exploring more environmental variables, such as seasonal changes or unique urban features could provide valuable insights. The conclusions drawn from this study can serve as a basis for future research.

- The engine showed higher supreme CP and heat release rate, with increases of approximately 70.84 bar and 36.65 CA, respectively, compared to CB20 at the standard compression ratio when the fuel

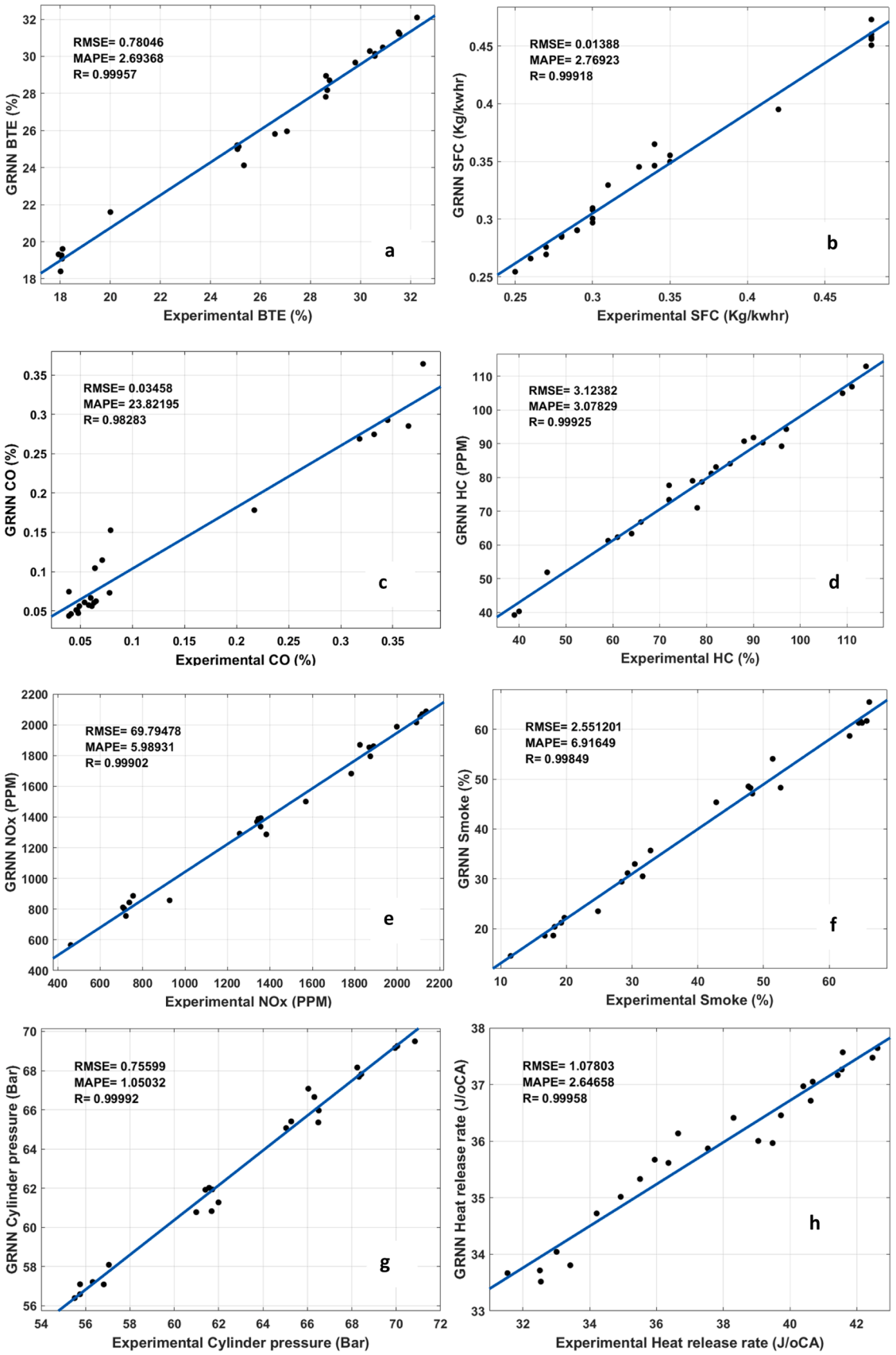

Fig. 12. GRNN predicted and experimental data: (a) GRNN predicted BTE vs. experimental BTE, (b) GRNN predicted SFC vs. experimental SFC, (c) GRNN predicted CO vs. experimental CO, (d) GRNN predicted HC vs. experimental HC, (e) GRNN predicted NOx vs. experimental NOx, (f) GRNN predicted smoke vs. experimental smoke, (g) GRNN predicted cylinder pressure vs. experimental cylinder pressure, (h) GRNN predicted heat release rate vs. experimental heat release rate.

Table 9
Correlation between predicted and measured values for engine characteristics (ECs) of novel ternary fueled engines.

ECs	Model equations	R^2
BTE model	$Y_{BTE} = 0.9057x + 2.4923$	0.968
SFC model	$Y_{SFC} = 1.000x - 0.0028$	0.952
CO model	$Y_{CO} = 1.1743x - 0.0252$	0.798
HC model	$Y_{HC} = 0.9025x - 7.5479$	0.914
NO_x model	$Y_{NOx} = 0.992x - 13.463$	0.9995
Smoke model	$Y_{Smoke} = 0.9469x + 2.1799$	0.9647
Cylindrical pressure model	$Y_{Smoke} = 0.9515x + 3.0399$	0.9874
Heat release rate	$Y_{HRR} = 0.9124x + 3.5766$	0.87411

x = input variable of the respective responses
y = response(s) of the model investigated

blend contained 120 ppm zinc oxide nano additive. Additionally, the supreme BTE and minimum SFC were observed as 31.56 % and 0.26 kg/kWh, respectively, with this fuel blend.

- The addition of zinc oxide nano additives also reduced CO and smoke emissions, with maximum decreases of 12.87 % and 1.86 %, respectively.
- An upsurge in NOx and HC emissions was noted with greater concentrations of the zinc oxide nano additive and CB20P5ZNO40 blends; however, these emissions were lower compared to blends without the additive.
- Linear equations were developed for GRNN -based predicted BTE, SFC, CO, NOx, Smoke, CP, HHR versus measured values with high regression coefficients ranging from 0.798 for the CO model to 0.9995 for NOx, demonstrating the utility of advanced neural network models in optimizing engine operations and enhancing environmental sustainability through informed fuel formulation and combustion optimization strategies.
- The GRNN successfully forecasted the outputs, as indicated by high R values in the range of 0.98284–0.99959, beside with lower RMSE and MAPE values, suggesting that the GRNN was within acceptable boundaries.
- This technique has proven effective for precisely forecasting engine efficiency and pollutant attributes of Calophyllum biodiesel along with propanol-2 and zinc oxide fuel additives in fuelled IC engines, reducing time waste and minimizing costs.

CRediT authorship contribution statement

PraveenKumar Seepana: Writing – review & editing, Investigation. **Samuel Olusegun D:** Writing – review & editing, Project administration, Investigation. **Mustafa Ahmad:** Writing – review & editing, Methodology. **Enweremadu Christopher C.:** Validation. **Elboughdiri Noureddine:** Writing – review & editing, Visualization. **M. Srinivasarao M.:** Writing – original draft, Visualization. **Srinivasarao Ch.:** Writing – original draft, Data curation. **Swarna Kumari A.:** Writing – original draft, Conceptualization. **Joga Bikkavolu:** Methodology, Investigation, Conceptualization. **Gandhi Pullagura:** Data curation, Conceptualization.

Declaration of Competing Interest

The authors declare that they have no known competing financial interests or personal relationships that could have appeared to influence the work reported in this paper.

Data availability

Data will be made available on request.

References

Aalam, C., Saravanan, C., 2017. Effects of nano metal oxide blended Mahua biodiesel on CRDI diesel engine. Ain Shams Eng. J. 8 (4), 689–696.

Abishek, M., Kachhap, S., Rajak, U., Verma, T., Singh, T., Shaik, S., Alwetaishi, M., 2024b. Alumina and titanium nanoparticles to diesel–Guizotia abyssinica (L.) biodiesel blends on MFVCR engine performance and emissions. Sustain. Energy Technol. Assess. 61, 103580.

Abishek, M., Kachhap, S., Rajak, U., Singh, T., Verma, T., 2024. Analysis and optimization of Guizotia abyssinica (L.) with alumina, titanium and diesel blends on DI engine combustion and emissions. Environ., Dev. Sustain. 1–26. https://doi.org/10.1007/s10668-024-04841-w.

Aengchuan, P., Wiangkham, A., Klinkaew, N., Theinnoi, K., Sukjit, E., 2022. Prediction of the influence of castor oil–ethanol–diesel blends on single-cylinder diesel engine characteristics using generalized regression neural networks (GRNNs). Energy Rep. 8, 38–47.

Atabani, A., da Silva César, A., 2014. Calophyllum inophyllum L.–A prospective non-edible biodiesel feedstock. Study of biodiesel production, properties, fatty acid composition, blending and engine performance. Renew. Sustain. Energy Rev. 37, 644–655.

Bendu, H., Deepak, B., Murugan, S., 2016. Application of GRNN for the prediction of performance and exhaust emissions in HCCI engine using ethanol. Energy Convers. Manag. 122, 165–173.

Bhuiya, M., Rasul, M., Khan, M., Ashwath, N., Azad, A., Hazrat, M., 2016. Prospects of 2nd generation biodiesel as a sustainable fuel–Part 2: Properties, performance and emission characteristics. Renew. Sustain. Energy Rev. 55, 1129–1146.

Bitire, S., Nwanna, E., Jen, T., 2023. The impact of CuO nanoparticles as fuel additives in biodiesel-blend fuelled diesel engine: A review. Energy Environ. 34 (7), 2259–2289.

Caraka, R., 2017. Modeling Crude Oil Prices (CPO) using General Regression Neural Network (GRNN). Int. J. Chem., Math. Phys. (IJCMP 1 (1), 62–67.

Caraka, R., 2017. Modeling crude oil prices (CPO) using general regression neural network (GRNN). Model. Crude Oil Prices. (CPO) Using Gen. Regres. Neural Netw. (GRNN). 1 (1), 62–67.

Celikoglu, H., 2006. Application of radial basis function and generalized regression neural networks in non-linear utility function specification for travel mode choice modelling. Math. Comput. Model. 44 (7-8), 640–658.

Celikoglu, H., Cigizoglu, H., 2007. Public transportation trip flow modeling with generalized regression neural networks. Adv. Eng. Softw. 38 (2), 71–79.

Devarajan, Y., Selvam, C., 2024. Utilization of Sterculia foetida oil as a sustainable feedstock for biodiesel production: optimization, performance, and emission analysis. Results Eng. 24, 103196.

Dhahad, H., Chaichan, M., 2020. The impact of adding nano-Al2O3 and nano-ZnO to Iraqi diesel fuel in terms of compression ignition engines' performance and emitted pollutants. Therm. Sci. Eng. Prog. 18, 100535.

El-Adawy, M., 2023. Effects of diesel-biodiesel fuel blends doped with zinc oxide nanoparticles on performance and combustion attributes of a diesel engine. Alex. Eng. J. 80, 269–281.

Hosseini, S., Taghizadeh-Alisaraei, A., Ghobadian, B., Abbaszadeh-Mayvan, A., 2017. Performance and emission characteristics of a CI engine fuelled with carbon nanotubes and diesel-biodiesel blends. Renew. Energy 111, 201–213.

Huang, Y., Wang, H., Zhang, X., Zhang, Q., Wang, C., Ma, L., 2022. Accurate prediction of chemical exergy of technical lignins for exergy-based assessment on sustainable utilization processes. Energy 243, 123041.

Jain, M., Chandrakant, U., Orsat, V., Raghavan, V., 2018. A review on assessment of biodiesel production methodologies from calophyllum inophyllum seed oil (doi:). Ind. Crops Prod. 114, 28–44. https://doi.org/10.1016/j.indcrop.2018.01.051.

Jayanthi, P., Rao, M., 2016. Effects of nanoparticles additives on performance and emissions characteristics of a DI diesel engine fuelled with biodiesel. Int. J. Adv. Eng. Technol. 9 (6), 689.

Kalaimurugan, K., Karthikeyan, S., Periyasamy, M., Mahendran, G., Dharmaprabhakaran, T., 2023. Experimental studies on the influence of copper oxide nanoparticle on biodiesel-diesel fuel blend in CI engine. Energy Sources, Part A: Recovery, Util., Environ. Eff. 45 (3), 8997–9012.

Kanimozhi, B., Karthikeyan, L., Praveenkumar, T., Alharbi, S., Alfarraj, S., Gavurová, B., 2023. Evaluation of karanja and safflower biodiesel on engine's performance and emission characteristics along with nanoparticles in DI engine. Fuel 352, 129101.

Kannan, G.R., Karvembu, R., Anand, R., 2011. Effect of metal based additive on performance emission and combustion characteristics of diesel engine fuelled with biodiesel. Appl. Energy 88 (11), 3694–3703.

Kulkarni, S., Chaudhary, A., Nandi, S., Tambe, S., Kulkarni, B., 2004. Modeling and monitoring of batch processes using principal component analysis (PCA) assisted generalized regression neural networks (GRNN). Biochem. Eng. J. 18 (3), 193–210.

Kumar, M., Gautam, R., Ansari, N., 2024. Optimisation of an experimental and feasibility research on a CRDI diesel engine based on a blend of waste cooking oil and waste plastic oil using RSM: A value addition for disposed waste oil (doi:). J. Energy Inst., 101564. https://doi.org/10.1016/j.joei.2024.101564.

Manigandan, S., Ponnusamy, V., Devi, P., Oke, S., Sohret, Y., Venkatesh, S., Gunasekar, P., 2020. Effect of nanoparticles and hydrogen on combustion performance and exhaust emission of corn blended biodiesel in compression ignition engine with advanced timing. Int. J. Hydrog. Energy 45 (4), 3327–3339.

McLellan, D., 2007. Application of a generalized regression neural network for nitrogen oxides monitoring. Dalhousie University, Halifax, Canada.

Montazer, G., Giveki, D., Karami, M., Rastegar, H., 2018. Radial basis function neural networks: a review. Comput. Rev. J. 1 (1), 52–74.

Mosarof, M., Kalam, M., Masjuki, H., Alabdulkarem, A., Habibullah, M., Arslan, A., Monirul, I., 2016. Assessment of friction and wear characteristics of Calophyllum

inophyllum and palm biodiesel (doi:). Ind. Crops Prod. 83, 470–483. https://doi.org/10.1016/j.indcrop.2015.12.082.
Najafi, G., 2018. Diesel engine combustion characteristics using nano-particles in biodiesel-diesel blends. Fuel 212, 668–678.
Nanthagopal, K., Ashok, B., Varatharajan, V., Anand, V., Dinesh Kumar, R., 2017. Study on the effect of exhaust gas-based fuel preheating device on ethanol–diesel blends operation in a compression ignition engine. Clean Technologies and Environmental Policy 19, 2379–2392.
Nema, V., Singh, A., Chaurasiya, P., Gogoi, T., Verma, T., Tiwari, D., 2023. Combustion, performance, and emission behavior of a CI engine fueled with different biodiesels: a modelling, forecasting and experimental study. Fuel 339, 126976.
Ni, Y., Li, M., 2016. Wind pressure data reconstruction using neural network techniques: A comparison between BPNN and GRNN. Measurement 88, 468–476.
Nithyananda, B., Prakash, G., Aradhya, V., Krishna, S., Vinay, K., Ankegowda, N., Imran, K., 2023. Prediction of responses for simarouba biodiesel based CRDI engine using general regression neural network. E3S Web Conf. 405, 02003.
Nour, M., Attia, A., Nada, S., 2019. Improvement of CI engine combustion and performance running on ternary blends of higher alcohol (Pentanol and Octanol)/hydrous ethanol/diesel. Fuel 251, 10–22.
Ong, H., Mahlia, T., Masjuki, H., Norhasyima, R., 2011. Comparison of palm oil, Jatropha curcas and Calophyllum inophyllum for biodiesel: a review. Renew. Sustain. Energy Rev. 15 (8), 3501–3515.
Padmanabhan, S., Devarajan, Y., Munuswamy, D., Sathiyamurthy, S., Selvam, C., 2024. Graphene-enhanced sustainable fuel from Calophyllum inophyllum for premixed charge compression ignition engines: Advancing circular economy and emission reduction. Results Eng. 24, 103096.
Permude, A., Pathak, M., Kumar, V., Singh, S., 2012. Influence of low viscosity lubricating oils on fuel economy and durability of passenger car diesel engine. SAE Int. J. Fuels Lubr. 5 (3), 1426–1435.
Polat, Ö., Yıldırım, T., 2008. Genetic optimization of GRNN for pattern recognition without feature extraction. Expert Syst. Appl. 34 (4), 2444–2448.
Pradeep, V., Jogarao, B., 2020. Production, perfomance and emisions of bio diesel from mixture of animal waste fats and degradation of bio diesel over time. Int. J. Innov. Technol. Explor. Eng. 9 (4), 2676–2681.
Pullagura, G., Vadapalli, S.V., Bikkavolu, J.R., Chebattina, K.R., 2023. Parametric study of GNPs nano addition in water diesel emulsified fuel on diesel engine at variable injection timings. Energy Sources, Part A: Recovery, Util. Environ. Eff. 45 (5), 7262–7279.
Qiao, L., Wang, Z., Zhu, J., 2020. Application of improved GRNN model to predict interlamellar spacing and mechanical properties of hypereutectoid steel. Mater. Sci. Eng.: A 792, 139845.
Rajak, U., Reddy, V., Ağbulut, Ü., Sarıdemir, S., Afzal, A., Verma, T., 2023. Modifying diesel fuel with nanoparticles of zinc oxide to investigate its influences on engine behaviors. Fuel 345, 128196.
Rajendran, S., Govindasamy, M., 2021. Effect of isopropyl alcohol on the performance, combustion and emission Characteristics variable compression ratio engine using rubber seed oil blends. Energy Sources, Part A: Recovery, Util., Environ. Eff. 1–16. https://doi.org/10.1080/15567036.2021.1887408.
Ramakrishnan, G., Krishnan, P., Rathinam, S., Devarajan, Y., 2019. Role of nano-additive blended biodiesel on emission characteristics of the research diesel engine. Int. J. Green. Energy 16 (6), 435–441.
Rangabashiam, D., Jayaprakash, V., Ganesan, S., Nagaraj, M., Rameshbabu, A., 2023. Emission, performance, and combustion study on nanoparticle-biodiesel fueled diesel engine. Energy Sources, Part A: Recovery, Util. Environ. Eff. 45 (3), 8396–8407.
Rao, M.S., Rao, C.S., Kumari, A.S., 2022. Synthesis, stability, and emission analysis of magnetite nanoparticle-based biofuels. J. Eng. Appl. Sci. 69 (1), 79.
Rooki, R., 2016. Application of general regression neural network (GRNN) for indirect measuring pressure loss of Herschel–Bulkley drilling fluids in oil drilling. Measurement 85, 184–191.
S. Gavhane, R., M. Kate, A., Pawar, A., Safaei, M., M. Soudagar, M., Mujtaba Abbas, M., Ahmed, W., 2020. Effect of zinc oxide nano-additives and soybean biodiesel at varying loads and compression ratios on VCR diesel engine characteristics. Symmetry 12 (6), 1042.
Samuel, O., Boye, T., Enweremadu, C., 2020. Financial and parametric study of biodiesel production from hemp and tobacco seed oils in modified fruit blender and prediction models of their fuel properties with diesel fuel. Bioresour. Technol. Rep. 12, 100599.
Samuel, O., Waheed, M., Taheri-Garavand, A., Verma, T., Dairo, O., Bolaji, B., Afzal, A., 2021. Prandtl number of optimum biodiesel from food industrial waste oil and diesel fuel blend for diesel engine. Fuel 285, 119049.
Sarma, C., Sharma, P., Bora, B., Bora, D., Senthilkumar, N., Balakrishnan, D., Ayesh, A., 2023. Improving the combustion and emission performance of a diesel engine powered with mahua biodiesel and TiO2 nanoparticles additive. Alex. Eng. J. 72, 387–398.
Sayin, C., Gumus, M., Canakci, M., 2012. Effect of fuel injection pressure on the injection, combustion and performance characteristics of a DI diesel engine fueled with canola oil methyl esters-diesel fuel blends. Biomass-.-. Bioenergy 46, 435–446.
Seela, C., Ravisankar, B., Raju, B., 2018. A GRNN based frame work to test the influence of nano zinc additive biodiesel blends on CI engine performance and emissions. Egypt. J. Pet. 27 (4), 641–647.
Seela, C., Ravi Sankar, B., Kishore, D., Babu, M., 2019. Experimental analysis on a DI diesel engine with cerium-oxide-added Mahua methyl ester blends. Int. J. Ambient Energy 40 (1), 49–53.
Shaafi, T., Sairam, K., Gopinath, A., Kumaresan, G., Velraj, R., 2015. Effect of dispersion of various nanoadditives on the performance and emission characteristics of a CI engine fuelled with diesel, biodiesel and blends—a review. Renew. Sustain. Energy Rev. 49, 563–573.
Sheriff, S., Kumar, I., Mandhatha, P., Jambal, S., Sellappan, R., Ashok, B., Nanthagopal, K., 2020. Emission reduction in CI engine using biofuel reformulation strategies through nano additives for atmospheric air quality improvement. Renew. Energy 147, 2295–2308.
Simhadri, K., Rao, P., Paswan, M., 2024. Improving the combustion and emission performance of a diesel engine with TiO2 nanoparticle blended Mahua biodiesel at different injection pressures. Int. J. Thermofluids 21, 100563.
Singh, D., Subramanian, K., Singal, S., 2015. Emissions and fuel consumption characteristics of a heavy duty diesel engine fueled with hydroprocessed renewable diesel and biodiesel. Appl. Energy 155, 440–446.
Singh, R., Singh, S., Kumar, M., 2020. Impact of n-butanol as an additive with eucalyptus biodiesel-diesel blends on the performance and emission parameters of the diesel engine. Fuel 277, 118178.
Soudagar, M., Afzal, A., Safaei, M., Manokar, A., EL-Seesy, A., Mujtaba, M., Goodarzi, M., 2020. Investigation on the effect of cottonseed oil blended with different percentages of octanol and suspended MWCNT nanoparticles on diesel engine characteristics. J. Therm. Anal. Calorim. 147, 1–18.
Suhel, A., Abdul Rahim, N., Abdul Rahman, M., Bin Ahmad, K., Teoh, Y., Zainal Abidin, N., 2021. An experimental investigation on the effect of ferrous ferric oxide nano-additive and chicken fat methyl ester on performance and emission characteristics of compression ignition engine. Symmetry 13 (2), 265.
Talam, S., Karumuri, S.R., Gunnam, N., 2012. Synthesis, characterization, and spectroscopic properties of ZnO nanoparticles. International Scholarly Research Notices 372505. https://doi.org/10.5402/2012/372505.
Tiwari, C., Verma, T., Dwivedi, G., 2024. Optimization of biodiesel production parameters for hybrid oil using RSM and ANN technique and its effect on engine performance, combustion, and emission characteristics. Proc. Inst. Mech. Eng., Part E: J. Process Mech. Eng. 09544089241241130.
Wolday, A., Ramteke, M., 2024. Surrogate model-based optimization of methanol synthesis process for multiple objectives: A pathway towards achieving sustainable development goals. Chem. Eng. Res. Des. 204, 172–182.
Xie, Y., Li, C., Lv, Y., Yu, C., 2019. Predicting lightning outages of transmission lines using generalized regression neural network. Appl. Soft Comput. 78, 438–446.
Yue, H., Bu, L., 2023. Prediction of CO2 emissions in China by generalized regression neural network optimized with fruit fly optimization algorithm. Environ. Sci. Pollut. Res. 30 (33), 80676–80692.